Flow Characteristics over Flat Building Roof with Different Edge Configurations for Wind Energy Harvesting: A Wind Tunnel Study

Shaopeng Li[1], Wei-Ting Lu[2], Brian M. Phillips[3*], and Zhaoshuo Jiang[4]

[1]Assistant Professor, Department of Civil Engineering,
Louisiana University at Lafayette, Lafayette, United States
[2]Postdoctoral Associate, Department of Civil and Coastal Engineering,
University of Florida, Gainesville, United States
[3]Associate Professor, Department of Civil and Coastal Engineering,
University of Florida, Gainesville, United States
[4]Associate Professor, Department of Civil and Environmental Engineering,
San Francisco State University, San Francisco, United States
[*]Corresponding author, brian.phillips@essie.ufl.edu

ABSTRACT: The impact of climate change and global warming makes it imperative to seek sustainable solutions for the built environment. To facilitate the design of future sustainable buildings, wind tunnel tests are conducted in this study to investigate the flow characteristics and wind energy potential over a flat building roof with different edge configurations. Specifically, this study addresses the effect of parapet walls and roof edge-mounted solar panels on the wind flow over a flat-roof tall building. The results show that parapet walls generally slow down the wind speed and increase turbulence intensity as well as skewness angle, which compromises the efficiency of traditional turbine-based wind energy harvesting. On the other hand, the presence of solar panels on the roof edge (or on the top of the parapet wall) further alters flow separation and has the potential to enhance wind energy harvesting over the roof, especially for the solar panel inclined at 30º. In addition to providing valuable data for validating computational fluid dynamics (CFD) simulations, this study could also help to guide the design of wind energy harvesting devices on the building roof and explore the promising synergy with solar panels.

KEYWORDS: wind energy; tall building; parapet wall; solar panel; wind tunnel test.

1 INTRODUCTION

Supported by the overwhelming scientific evidence, climate change has long been recognized as a serious phenomenon with severe implications for the planet, its inhabitants, and the built environment (Moss *et al.,* 2010; IPCC, 2023), which motivates researchers to seek sustainable solutions. One effective strategy for climate mitigation is to exploit renewable energy to replace fossil fuel (Ellabban *et al.,* 2014). For example, deployment of energy harvesting devices on buildings (e.g., solar panel and wind turbine) is a promising approach to achieve net-zero emission, considering the convenient use of on-site energy and the reduced cost on power transmission/distribution (Ahmed *et al.,* 2022). Recently, there are growing interests in utilizing wind energy around tall buildings in urban areas due to the high power demand and rich energy potential (Stathopoulos et al., 2018; Toja-Silva et al., 2018; Vita et al., 2020a; Škvorc and Kozmar, 2021; Kwok and Hu, 2023). Efforts have been made to investigate the performance of various wind energy harvesting systems on urban buildings such as wind turbines (e.g., Li et al., 2013), power windows (e.g., Jafari et al., 2019), vibration-based energy harvesters (e.g., Abdelkefi, 2016), and innovative building façades (e.g., Hassanli et al., 2017). Among them, wind turbines (with horizontal axis and vertical axis) are currently most popular (Kumar et al., 2018; Anup et al., 2019), and have been implemented in real urban buildings (e.g., Bahrain World Trade Center). These systems can be implemented on rooftops, in through-building openings, on building sides, or between two buildings. Among the various possibilities, implementing wind energy harvesting systems on a building roof is relatively easy (although the overturning moment of the device and the added load on the building need to be carefully analyzed for practical implementation). In addition, roof-mounted energy systems can be introduced to existing buildings, which hence has promising potential for wide applications. As a result, it is of great importance to systemically investigate the flow characteristics over the building roof to inform the practical design of wind energy harvesting devices.

Several researchers have studied the wind energy potential over the roofs of tall buildings based on numerical simulation and/or experimental testing. Toja-Silva et al. (2013) used computational fluid dynamics (CFD) simulation based on Reynolds-averaged Navier–Stokes equations (RANS) to investigate the wind energy potential on an isolated building with flat roof, where the performances of horizontal-axis wind turbines and vertical-axis wind turbines were compared. Later, CFD simulations with different turbulence models for RANS were conducted to assess the energy potential for different regions over the building roof (Toja-Silva *et al.,* 2015a). Kono et al. (2016) utilized CFD simulations, specifically, large eddy simulation (LES), to study the effects of wind direction and aspect ratio of a high-rise building for roof-mounted wind turbines. Peng et al. (2020) conducted wind tunnel tests to investigate the wind energy potential over tall building roof, where the effects of building's height ratio and width ratio are examined. Moving from a single building to multiple buildings, Lu and Ip (2009) adopted CFD simulations (RANS) to empirically investigate the feasibility of enhancing power generation through strategic arrangement of building cluster. Wang et al. (2015) evaluated the wind energy over the roof of two perpendicular buildings using CFD simulations (RANS), which considered different factors in terms of building lengths, widths, heights, corner separation distances, angles of inlet and altitudes of assessment. Glumac et al. (2018) conducted wind tunnel tests to investigate the impact of four neighboring buildings on the wind energy potential above a high-rise building, accompanied by roof pressure measurement on the principal building. In addition, CFD simulations (RANS) of generic high-rise building arrays have been conducted to study the impact of building layout parameters such as urban densities and staggered patterns (Juan *et al.,* 2021; Juan *et al.,* 2022). Noting that building shapes can greatly impact the flow field, attempts have also been made to investigate wind energy potential for buildings shapes beyond standard cuboids. Dai et al. (2022a) utilized CFD simulations (RANS) to study the effects of corner modifications for tall buildings, where, compared to benchmark and recessed corners, rounded and chamfered corners are found to be more promising for the installation of wind turbines due to the higher wind velocity and lower turbulence intensity. Dai et al. (2022b) studied the effect of parapet wall height on wind energy potential over tall building roofs using CFD simulation (RANS), revealing the importance of considering parapet wall for wind energy harvesting applications. In addition to flat roofs in abovementioned studies, Toja-Silva et al. (2016) conducted CFD simulation (RANS) to explore the wind energy potential of novel shapes of roof (e.g., spherical roof) and empirically optimized the building roof geometry for harvesting wind energy on high-rise buildings.

Despite the merits of being clean and renewable, the intermittent nature of wind makes it difficult to consistently meet the power demand of the building, and hence it is desirable to have multiple energy sources for sustainable buildings. A hybrid wind-solar energy harvesting system is a promising direction, considering the complementarity of technology and stability of power generation (Hong and Chen, 2014; Sinha *et al.,* 2021). Specifically, solar irradiation is available during the day, while the wind energy supply during the night is at its highest. In addition, the availability of solar power is higher than wind in the summer, while the opposite is true in the winter (Liu and Wang, 2009; Huang *et al.,* 2015). It should be noted that mounting solar panels on the building roof can modify the aerodynamic shape and hence affect the wind energy potential. Most of existing research on roof-mounted solar panel focuses on the aerodynamic loads (e.g., Stathopoulos *et al.,* 2014; Dai *et al.,* 2022c), while only a few studies reveal the flow characteristics over the solar panel (Pratt and Kopp, 2013; Toja-Silva *et al.,* 2015b; Wang *et al.,* 2020). Pratt and Kopp (2013) conducted wind tunnel tests to better understand the flow structures and aerodynamic mechanisms for peak wind loads for roof-mounted solar arrays using synchronized particle image velocimetry (PIV) and pressure measurements. Toja-Silva et al. (2015b), from the view of the wind energy exploitation, performed CFD simulation (RANS) to investigate flow characteristics over the roof-mounted solar panels with two different tilting angles (10º and 30º). Aiming to clarify the relations between flow field and wind pressure distributions on solar panels, Wang et al. (2022) conducted CFD simulations (LES) to examine the flow characteristics around solar arrays mounted on a flat-roof building for two wind directions (0º and 180º). It should be noted that in the abovementioned studies the solar panels are located away from the roof edge. Hence, the impact on wind energy potential over building roof (for wind energy harvesting devices located at a much higher elevation than the solar panel) is not significant, considering that the rooftop flow field is mainly controlled by the flow separation at the roof edge.

Noting the significant impact of flow separation at the roof edge on wind energy potential, this study investigates flow characteristics over a flat building roof with different edge configurations through wind tunnel tests. Specifically, this study utilizes velocity probes to characterize the wind flow over a tall building's flat roof, considering different heights of parapet walls and tilting angles of solar panels mounted on the roof edge. Noting that the solar panels can also be used to adaptively change the roof shape for wind energy harvesting, the scenario of solar panels mounted on the top of the parapet wall is also considered to further demonstrate the concept. In the following sections, the experiment setup is first introduced, which is followed by a detailed result analysis. The concluding remarks and future directions are given at the end. This study can effectively contribute to (1) providing valuable data for validating CFD simulations, (2) guiding the design of hybrid wind-solar energy harvesting systems on building roofs, and (3) exploring the promising potentials to develop "morphing" roofs using active devices for maximizing wind (and/or solar) power generation.

2 EXPERIMENT SETUP

2.1 Model configuration

In this study, building models with nine different configurations are tested in the wind tunnel (see Fig. 1). The models include one baseline model, two models with a parapet wall, three models with solar panels, and three models with both a parapet wall and solar panels. The baseline model has the dimension of 500mm × 500mm × 1000mm (aspect ratio 1:1:2), which, using the length scale of 1:50, corresponds to a 50m tall building in full scale. To investigate the effect of parapet walls on rooftop flow characteristics and wind energy potential, two different heights of parapet walls are considered in this study, which are 20mm and 40mm (1m and 2m in full scale). To investigate the impact of the solar panel on wind energy potential, this study considers two scenarios with different mounting locations. In the first scenario, the solar panel with a width of $40\sqrt{2}$mm and a length of 400mm (4/5 of the building's side dimension) is mounted on the roof edge with three tilting angles (15°, 30° and 45°), in contrast with existing studies that mount solar panel away from the roof edge (Pratt and Kopp, 2013; Toja-Silva *et al.,* 2015b; Wang *et al.,* 2020). In the second scenario, the solar panel (with the same dimension) with three tilting angles (15°, 30° and 45°) is mounted on the top of the parapet wall (with 40mm wall height), where the solar panel can also be considered as a potential active device to adaptively change the aerodynamic shape of the building. It is noted that this study only focuses on the wind energy potential, while the wind load on the solar panels needs to be investigated in future studies.

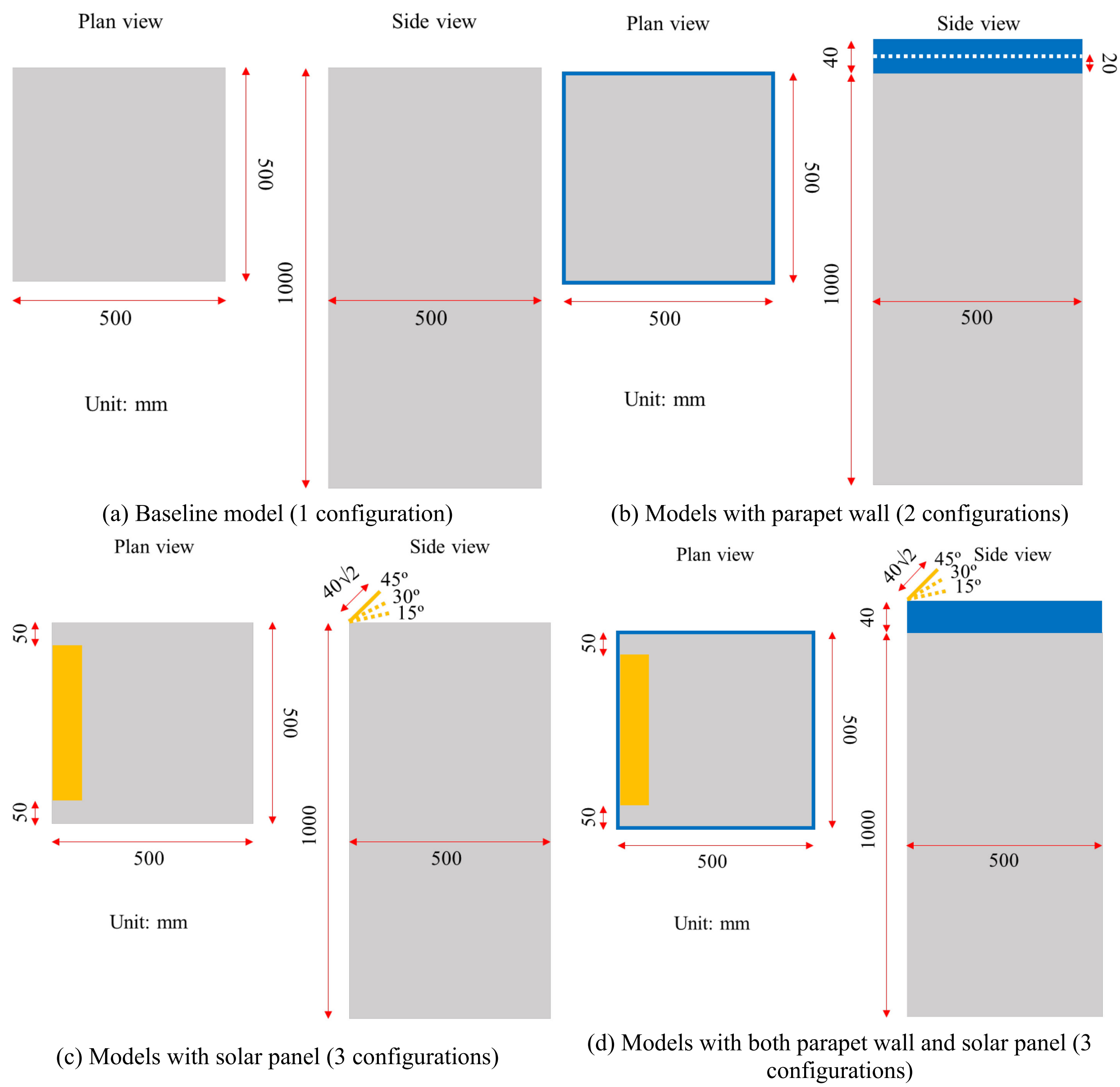

Figure 1. Configurations of nine building models with different roof edge configurations

2.2 Wind tunnel and sensor instrumentation

The wind tunnel tests are conducted in the Natural Hazards Engineering Research Infrastructure (NHERI) experimental facility (EF) at the University of Florida (UF), which is funded by National Science Foundation (NSF). The UF boundary layer wind tunnel (BLWT) is a long-fetch low-speed open circuit tunnel with the dimension of 6 m (width) × 3 m (height) × 38 m (length) (see Fig. 2). In the UF BLWT, eight vane axial fans generate the axial flow passing honeycomb and Irwin spires. The terrain condition is automatically controlled by the Terraformer, an array of 1116 electronically actuated roughness element assemblies that independently rotate and translate to precisely control height and aspect ratio. Roughness extension grid is added after the end of Terraformer to avoid rapid change in mean wind speed and turbulence intensity after transitioning into the smooth floor. The model under testing is located at the center of the turntable, which is 31.5m downwind of the vane axial fans. Detailed descriptions of the UF BLWT configuration and capability can be found in (Catarelli *et al.,* 2020a and 2020b). Turbulent flow fields in the wind tunnel are measured with the help of an automated multi-degree-of-freedom instrument gantry, which is capable of traversing longitudinally, laterally, and vertically. The gantry system is equipped with multiple Vectoflow cobra probes that can simultaneously measure the three velocity components of the turbulent winds (Vectoflow). As shown in Fig. 3, the wind flow above the five locations in the model centerline (with 80mm interval) is measured from the elevation of 1100mm (55m in full scale) to 1650mm (82.5m in full scale) at 50mm intervals (2.5m in full scale). Specifically, the velocity measurements at 12 vertical locations are realized by two independent measurements using six probes with a 100mm gap (i.e., the gantry was moved 50mm upward for second measurement). The probes have an acceptance cone of ± 60º, so data quality will drop if placed into the near-roof recirculation zone (with reverse flow). For the sake of completeness, the data quality of the wind speed measurements in this study is discussed in the Appendix. PIV or CFD may be needed to accurately characterize the flow recirculation zone, which, however, is beyond the scope of this study. Only 0º wind direction is considered in this pilot study for effective comparison of the flow characteristic for different roof edge configurations, while a wide range of wind directions are intended to be considered in the future for practical implementation of wind harvesting devices. The setup in the wind tunnel is shown in Fig. 4. The sampling frequency of the Vectoflow probes are set to 850Hz and the sampling duration is 120s.

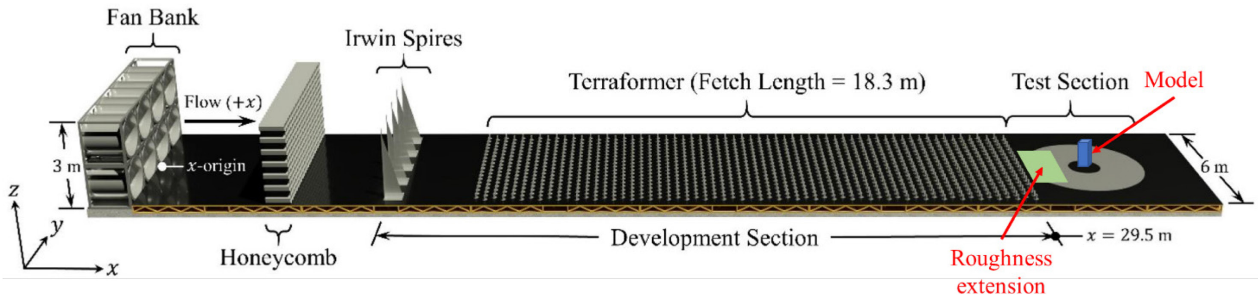

Figure 2. Configuration of UF BLWT

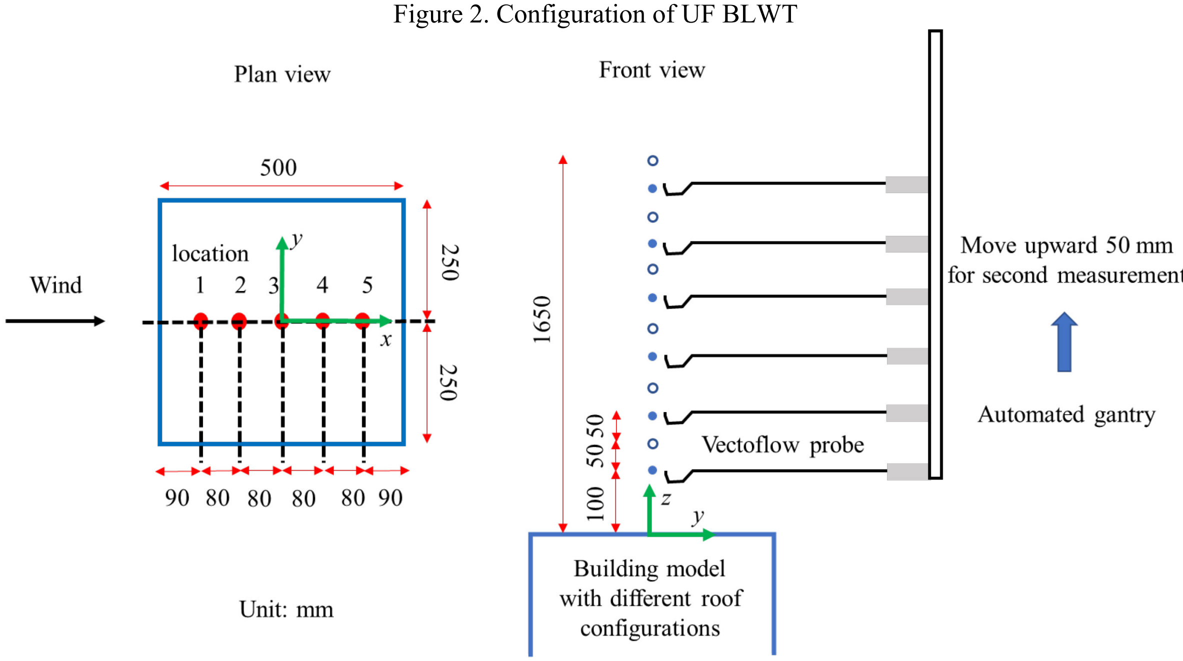

Figure 3. Sensor instrumentation for wind speed measurement over building roof

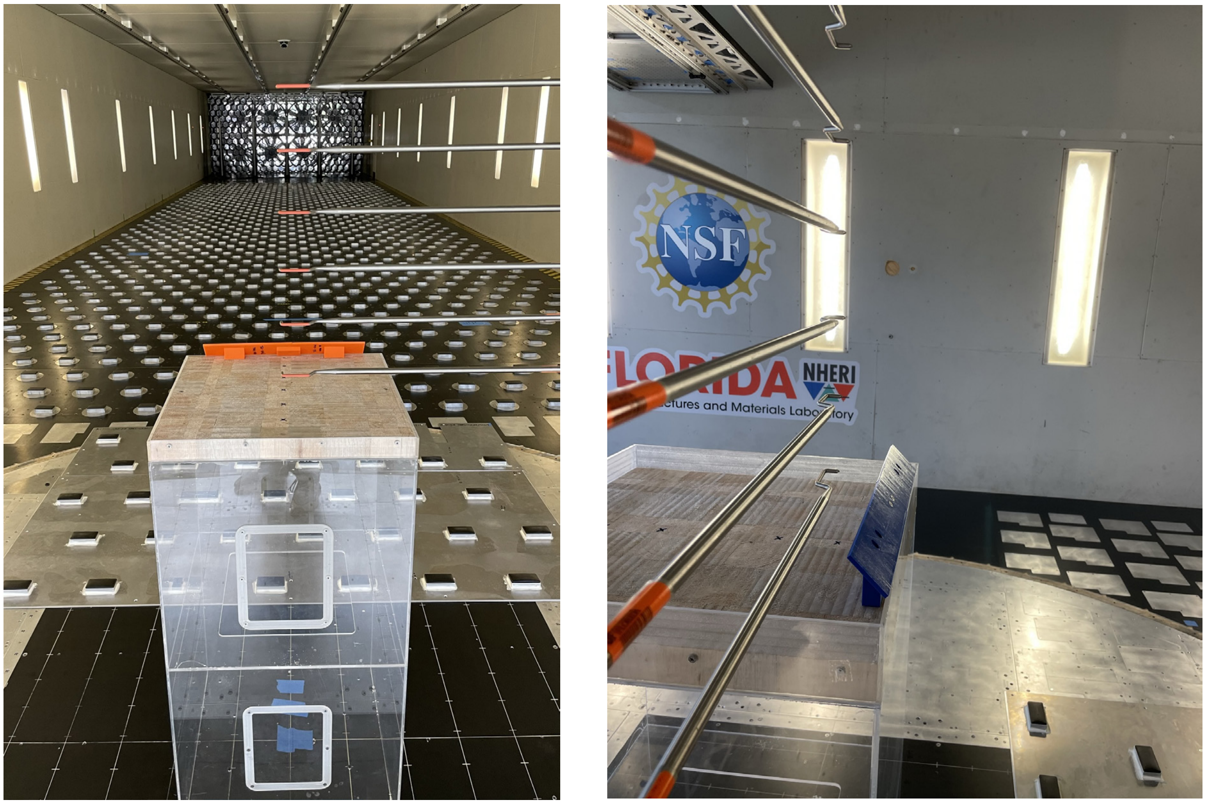

(a) Front view (b) Side view

Figure 4. Experiment setup in the wind tunnel

3 RESULT ANALYSIS

The approach flow condition in the wind tunnel is schematically shown in Fig. 5, where the mean wind speed *U* at different elevations *z* (without model) is normalized by the reference wind speed U_{ref} = 11.5m/s at the reference height H = 1m (note that 1m is the height of the model). The target approach flow condition was "open terrain" (power law with $\alpha = 0.1$), which corresponds to the case of a tall building located on flat terrain with good wind energy potential for common turbine-type devices (e.g., near a lake or ocean). It is noted that different types of wind energy harvesting devices (e.g., horizontal/vertical-axis wind turbines and vibration-based wind energy harvesters) can be implemented on the building roof, and their requirements on the wind characteristics may vary from case to case (Kumar et al., 2018; Anup et al., 2019; Lai et al., 2021), which needs detailed analysis for each scenario. In addition, only the open terrain condition is considered in the wind tunnel experiment, while the effect of incoming turbulence, which is important for urban setting (e.g., Vita et al., 2020b), requires further investigations in future work. For the sake of general applications, the study selects the mean wind speed in longitudinal direction U, its turbulence intensity I_u and the skewness angle θ [$\theta = \arctan(W/U)$ reflecting the change of wind direction] as the three main indicators for wind energy potential. In addition, it is assumed that higher values of U and lower values of I_u and θ are generally desirable for turbine-type wind energy harvesting devices. The flow characteristics over the roof of the baseline model, in terms of the three indicators U, I_u and θ are respectively shown in Fig. 6(a)-(c), while the vector-based representation of mean flow field over the five longitudinal measurement locations (x/B = -0.32, -0.16, 0, 0.16, 0.32; x is coordinate in along wind direction with origin at building roof center; B is the width of the building) is schematically shown in Fig. 6(d). From the change in mean wind speed U, the development of boundary layer over the building roof can be observed in terms of deaccelerating the flow along the x direction. On the other hand, the variation in the skewness angle θ shows the flow separation near the windward edge (based on positive values of θ at location 1 and 2) and reattachment near the leeward edge (based on negative values of θ at location 3, 4 and 5). These typical characteristics of bluff-body aerodynamics can also be clearly observed in the vector-based mean flow field. Regarding the turbulence intensity, I_u generally increases with the fetch. The variations in different locations become negligible above the elevation around z/H=1.30 (15m above the roof in full scale) and the turbulence intensity is close to open flow condition. In the following sections, the impacts of parapet wall and solar panel (mounted on the roof edge and on the parapet wall) on the wind field are presented in detail and the implications on wind energy potential are discussed.

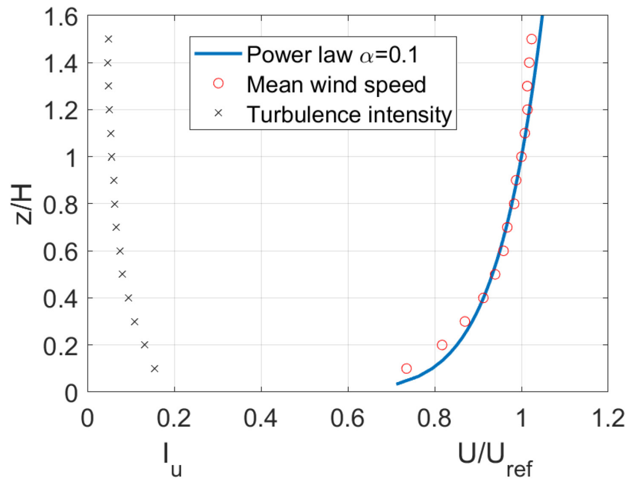

Figure 5. Approach flow condition at the model location

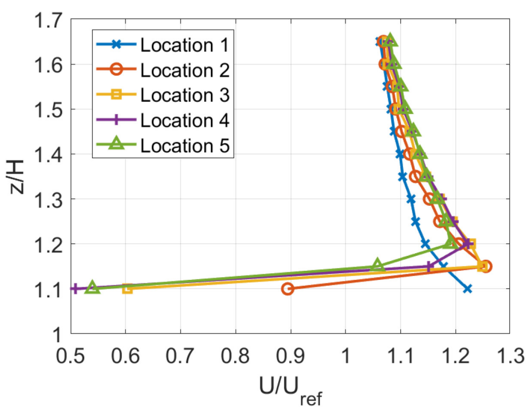

(a) Mean wind speed U

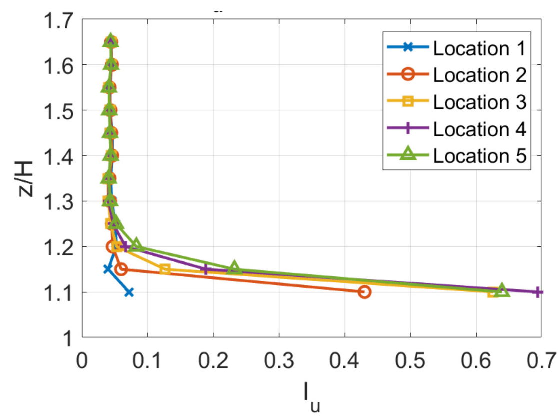

(b) Turbulence intensity I_u

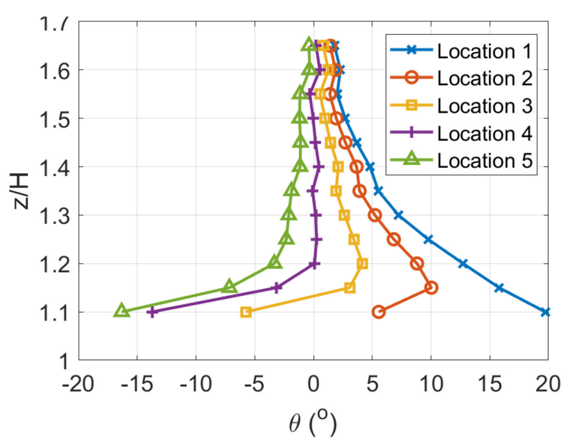

(c) Skewness angle θ

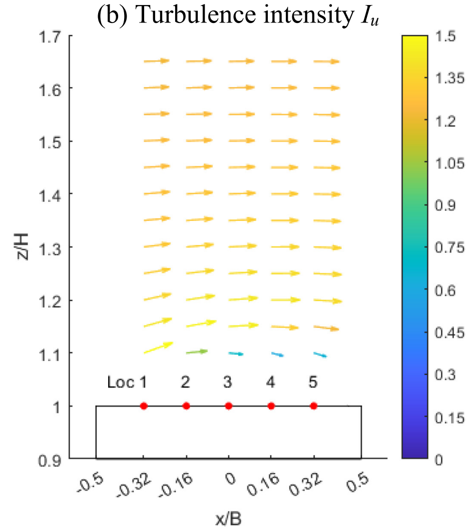

(d) Vector-based mean wind field

Figure 6. Rooftop wind field above the five locations of baseline model

3.1 Effect of parapet wall on flow characteristics and wind energy potential

To illustrate the effect of parapet wall on flow characteristics, the rooftop wind fields for models with 20mm and 40mm parapet wall are compared with baseline model. The mean wind speed U, turbulence intensity I_u and the skewness angle θ at the five measurement locations are shown in Fig. 7, followed by the vector-based mean flow field in Fig. 8. Compared with the baseline model, the mean wind speed U generally decreases near the roof due to the existence of parapet wall, while a slight increase in U is observed at higher elevations for the leeward side (location 3, 4 and 5). Regarding the turbulence intensity, I_u near the roof increases significantly due the existence of parapet wall for all five measurement locations, and the threshold elevation (above which the impact of parapet wall on I_u is small) generally increases with the fetch. In addition, the parapet wall tends to increase the absolute value of skewness angle θ, especially for higher elevations of windward locations and lower elevations of leeward locations. As also observed from vector-based representation in Fig. 8, the parapet wall in fact has the effect of "lifting up" the flow over building roof, and a larger "lift-up" effect occurs with a higher parapet wall.

Noting the significant impact of parapet wall on flow characteristics, the obtained results can also be used to inform the practical design of wind energy harvesting systems on the roof of tall buildings. Generally speaking, the existence of parapet wall has negative impacts on wind energy potential, considering (1) the reduced mean wind speed U near the roof will result in low wind power, (2) the increased skewness angle θ may cause misalignment between the wind direction and the wind energy harvesting device, (3) the increased turbulence intensity I_u can lead to low power generation efficiency as well as fatigue issues for common wind energy harvesting devices, and (4) the potential need to increase in the elevation of wind energy harvesting devices (e.g., hub height) to accommodate the "lift-up" effect may result in higher installation costs. To clearly show the impact of parapet wall on the wind energy potential, the flow characteristics at z

= 1.10H, 1.15H and 1.20H (5m, 7.5m and 10m above the roof in full scale), as typical installation heights of wind energy harvesting devices, are shown in Fig. 9. It is observed that a higher parapet wall leads to a lower mean wind speed U near the roof for z = 1.10H and 1.15H, while the impact become less significant at a higher elevation for z = 1.20H. Regarding turbulence intensity, the existence of parapet wall can effectively increase I_u for all three elevations. In addition, the effect of parapet become more obvious as the fetch increases. For the skewness angle, parapet wall can generally reduce the absolute value of θ for z = 1.15H and 1.20H, while a clear trend is not available near the roof at z = 1.10H. In addition to the flow characteristics at the three fixed elevations, the minimum hub heights h_{min} of typical horizontal-axis wind turbines for the five measurement locations are also calculated as a metric for wind energy potential, which are shown in Fig. 10. Specifically, the minimum hub height h_{min} in this study is selected as the threshold elevation, above which the turbulence intensity in the longitudinal direction I_u is below 15% (note that linear interpolation is used to determine h_{min}). The threshold value of 15% is adopted based on the specification in European Wind Turbine Standards II (Pierik *et al.,* 1999), which suggests that the fatigue loads on the wind turbines should be reevaluated based on the actual flow conditions at the site if the turbulence intensity exceeds 15%. The metric of minimum hub height h_{min} has also been used in other existing studies for rooftop wind energy potential (e.g., Toja-Silva *et al.,* 2015a; Peng *et al.,* 2020). It is clear from Fig. 10 that the minimum hub height h_{min} monotonically increases with the fetch, which indicate that a higher turbine is required at the leeward side. In addition, h_{min} increases with the height of parapet wall, indicating that taller wind turbines (and hence higher cost) are needed for buildings with higher parapet walls.

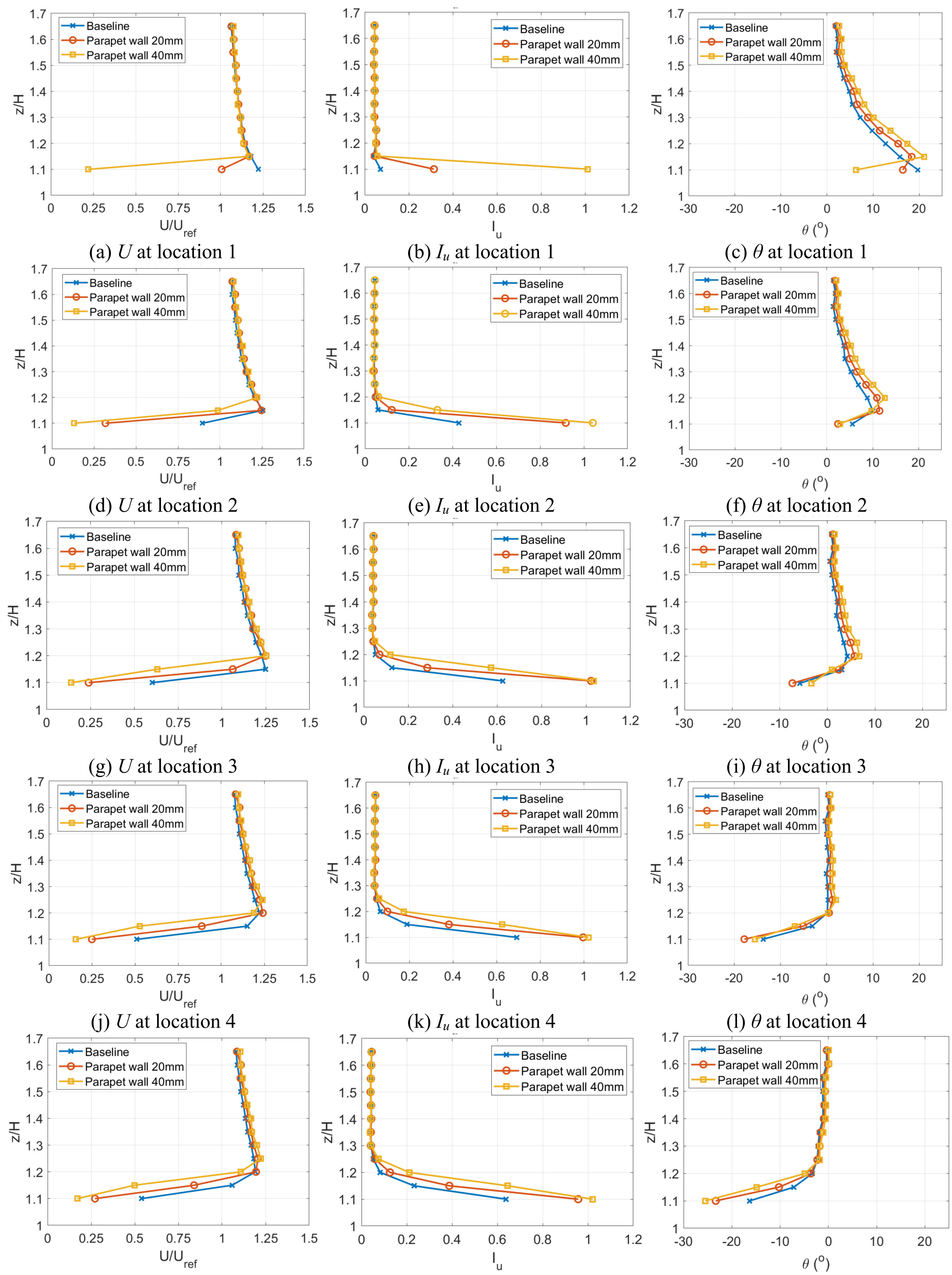

(a) U at location 1 (b) I_u at location 1 (c) θ at location 1

(d) U at location 2 (e) I_u at location 2 (f) θ at location 2

(g) U at location 3 (h) I_u at location 3 (i) θ at location 3

(j) U at location 4 (k) I_u at location 4 (l) θ at location 4

(m) U at location 5 (n) I_u at location 5 (o) θ at location 5

Figure 7. Rooftop flow characteristics for models with parapet wall

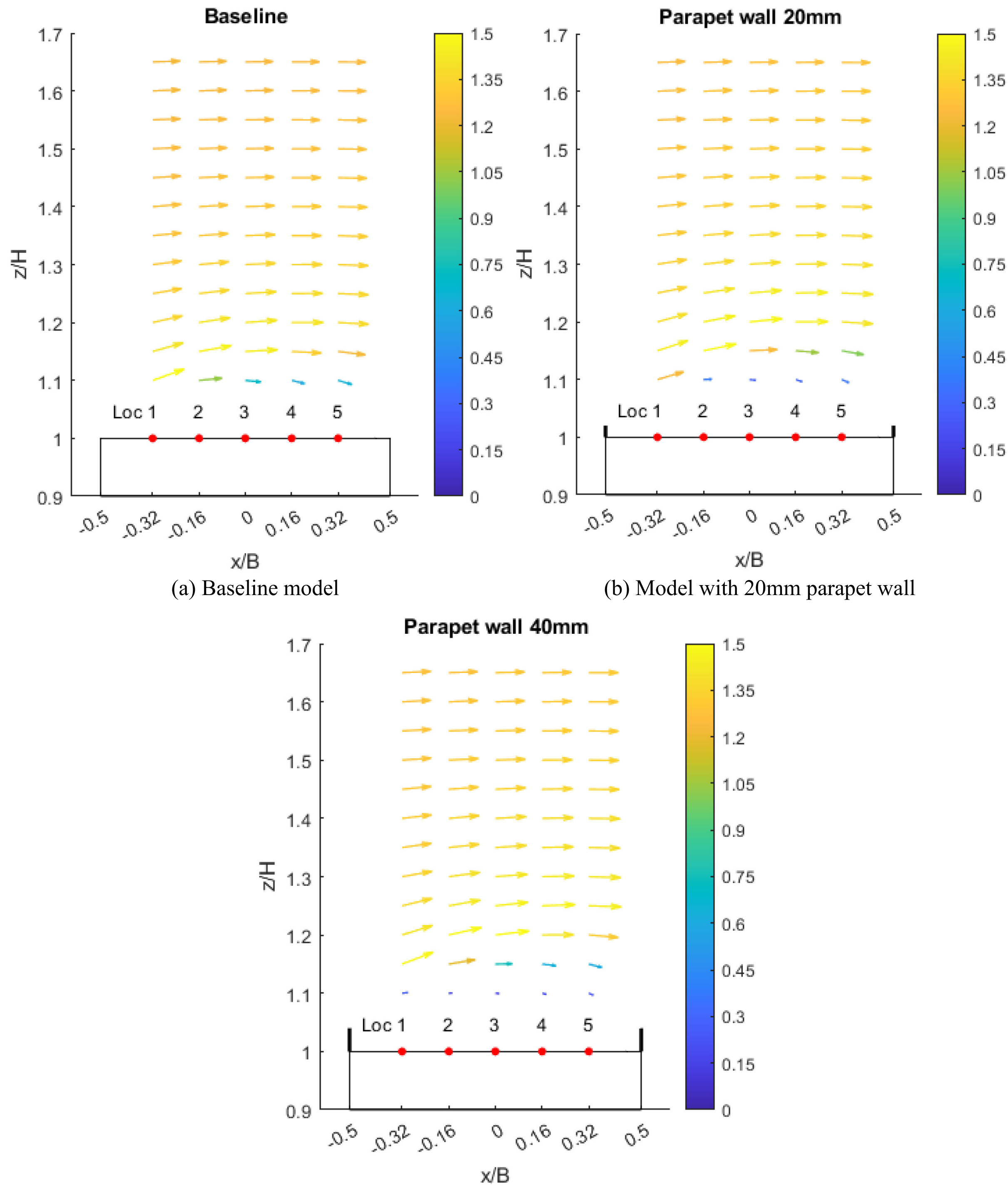

(a) Baseline model

(b) Model with 20mm parapet wall

(c) Model with 40mm parapet wall

Figure 8. Vector-based mean wind field for models with parapet wall

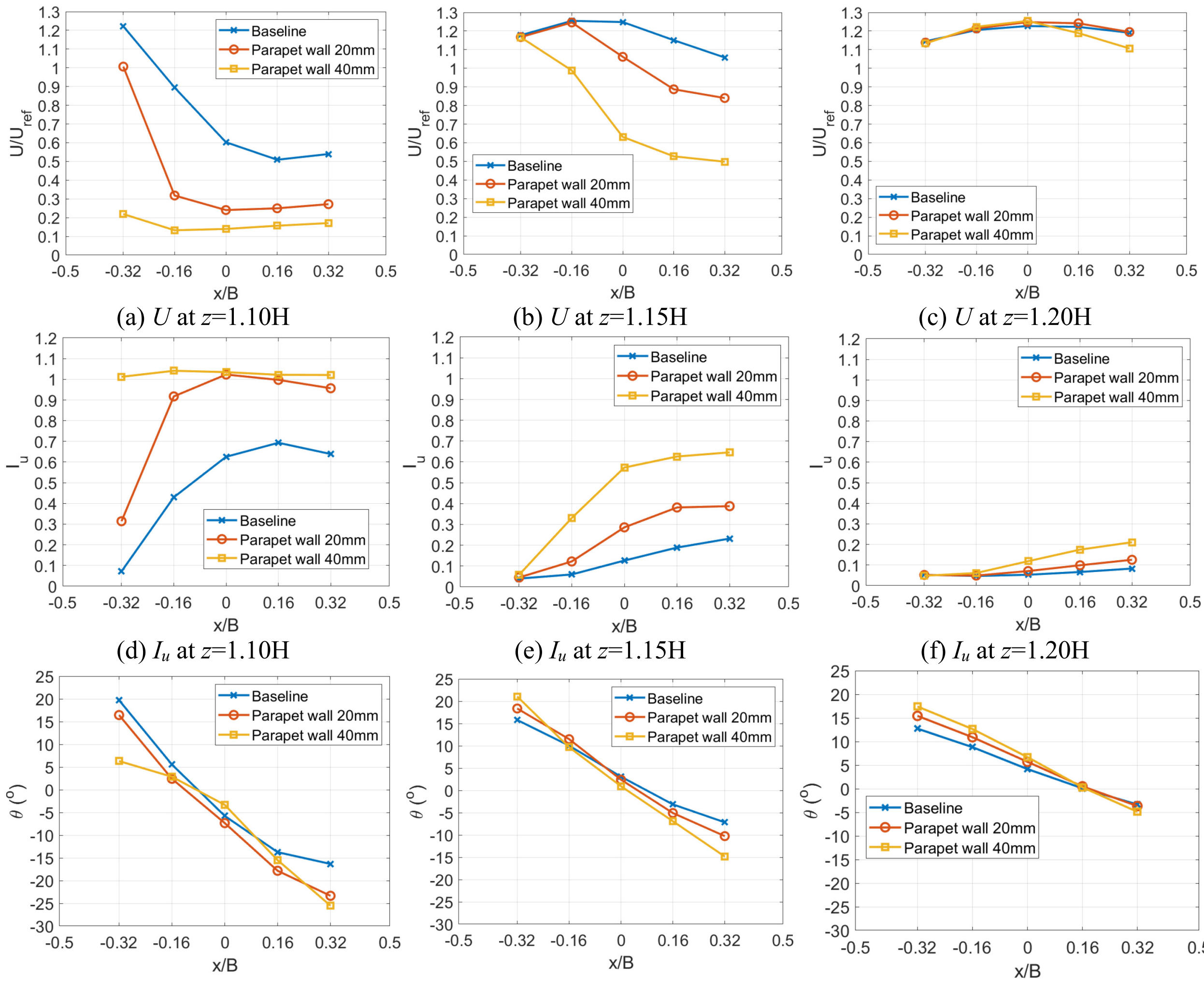

(a) U at z=1.10H (b) U at z=1.15H (c) U at z=1.20H

(d) I_u at z=1.10H (e) I_u at z=1.15H (f) I_u at z=1.20H

(g) θ at z=1.10H (h) θ at z=1.15H (i) θ at z=1.20H

Figure 9. Impact of parapet wall on wind energy potential at z=1.10H, 1.15H and 1.20H

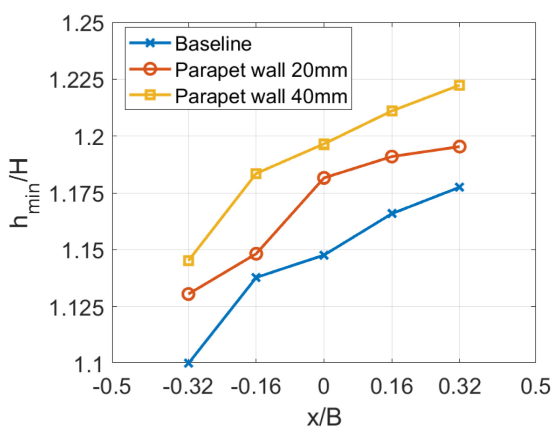

Figure 10. Impact of parapet wall on minimum hub height h_{min}

3.2 Effect of solar panel on flow characteristics and wind energy potential

3.2.1 *Solar panel mounted on roof edge*

To illustrate the effect of solar panels on flow characteristics, the rooftop wind fields for models with solar panels mounted on the roof edge (tilted at 15º, 30º and 45º) are compared with baseline model at the five measurement locations. The mean wind speed *U*, turbulence intensity I_u and the skewness angle θ are shown in Fig. 11, followed by the vector-based flow representation in Fig. 12. It is observed that the model with solar panel tilted at 15º has a very similar wind field in terms of both mean wind speed and turbulence intensity as the baseline model, indicating that 15º tilting angle is too small to significantly modify the flow field. On the other hand, solar panel with 30º and 45º tilting angle can effectively change the flow field. For the solar panel with 45º tilting angle, reduced mean wind speed *U* is identified near the roof. Skewness angle θ generally increases at most of elevations for the windward side (location 1, 2 and 3), while reduced θ is found near the roof for the leeward side (location 4 and 5). For turbulence intensity, increases in I_u can be observed near the roof. In contrast to solar panel with 45º tilting angle, larger *U* is observed near the roof for 30º tilted solar panel. Smaller I_u and θ, compared to that of the baseline model, are clearly observed for almost all measurement locations and elevations. These interesting features for 30º tilting angle indicate that the angle of 120º, formed by the building edge and 30º tilted solar panel, can effectively mitigate flow separation on the roof edge.

To clearly show the impact of solar panel on wind energy potential, the flow characteristics of three typical elevations at z = 1.10H, 1.15H and 1.20H are shown in Fig. 13. As mentioned previously, the solar panel with 15º tilting angle has relatively small impacts on the flow field, while 45º and 30º degree tilting angles generally have opposite effects on wind energy potential. For z=1.10H, it is clear that solar panel with 30º can significantly increase the mean wind speed *U* and reduce the turbulence intensity I_u as well as skewness angle θ, while the opposite is true for

45º tilting angle. The superiority of 30º over 45º tilting angle becomes less significant as the elevation increases. For z=1.15H, the 45º tilted solar panel, although have negligible effects on U and I_u, may compromise wind energy potential due to increase in skewness angle θ for windward side (location 1, 2 and 3). In contrast, the 30º tilted solar panel can effectively enhance wind energy potential, considering the increase in U (for location 4 and 5) and decrease in θ (for all five locations) as well as I_u (for location 3, 4 and 5). For z=1.20H, the differences among the models with various tilting angle become almost indistinguishable, except for the slight increase in θ caused by the 45º tilted solar panel and the slight decrease in θ caused by the 30º tilted solar panel. The minimum hub heights h_{min} of horizontal-axis wind turbines are shown in Fig. 14 for solar panels with different tilting angles. While solar panel with 30º and 45º tilting angle have nearly the same h_{min} as that of the baseline, the 30º tilted solar panel can significantly reduce h_{min} for all locations and hence have the lowest installation cost among other alternatives.

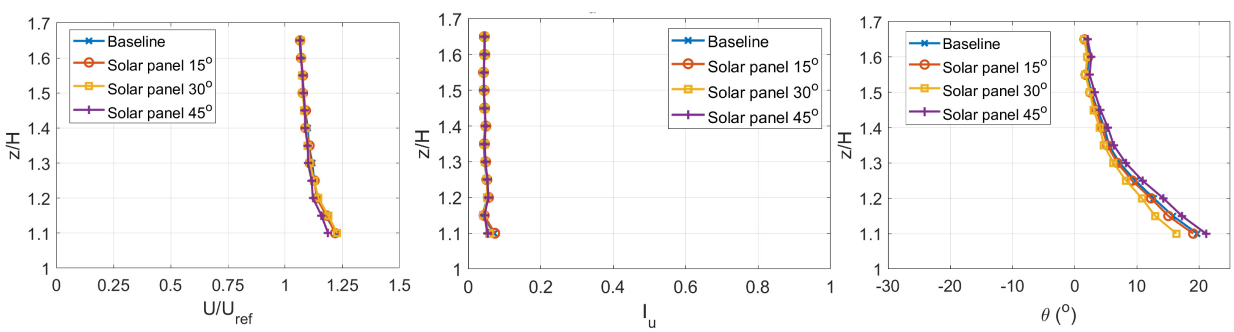

(a) U at location 1 (b) I_u at location 1 (c) θ at location 1

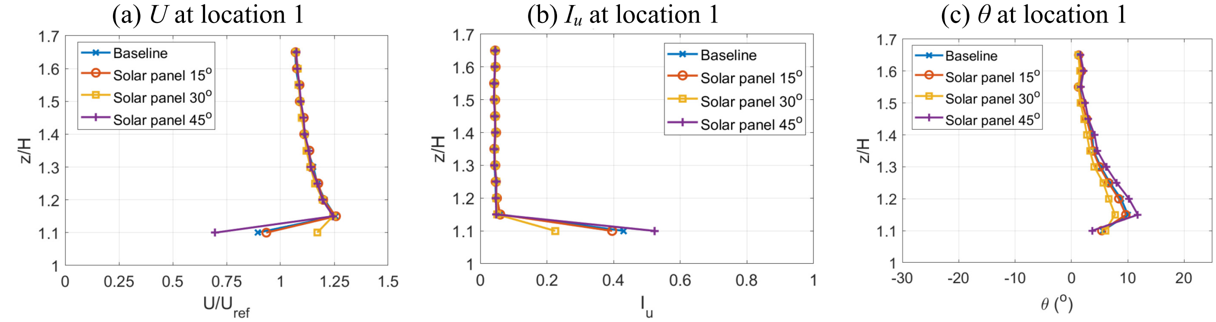

(d) U at location 2 (e) I_u at location 2 (f) θ at location 2

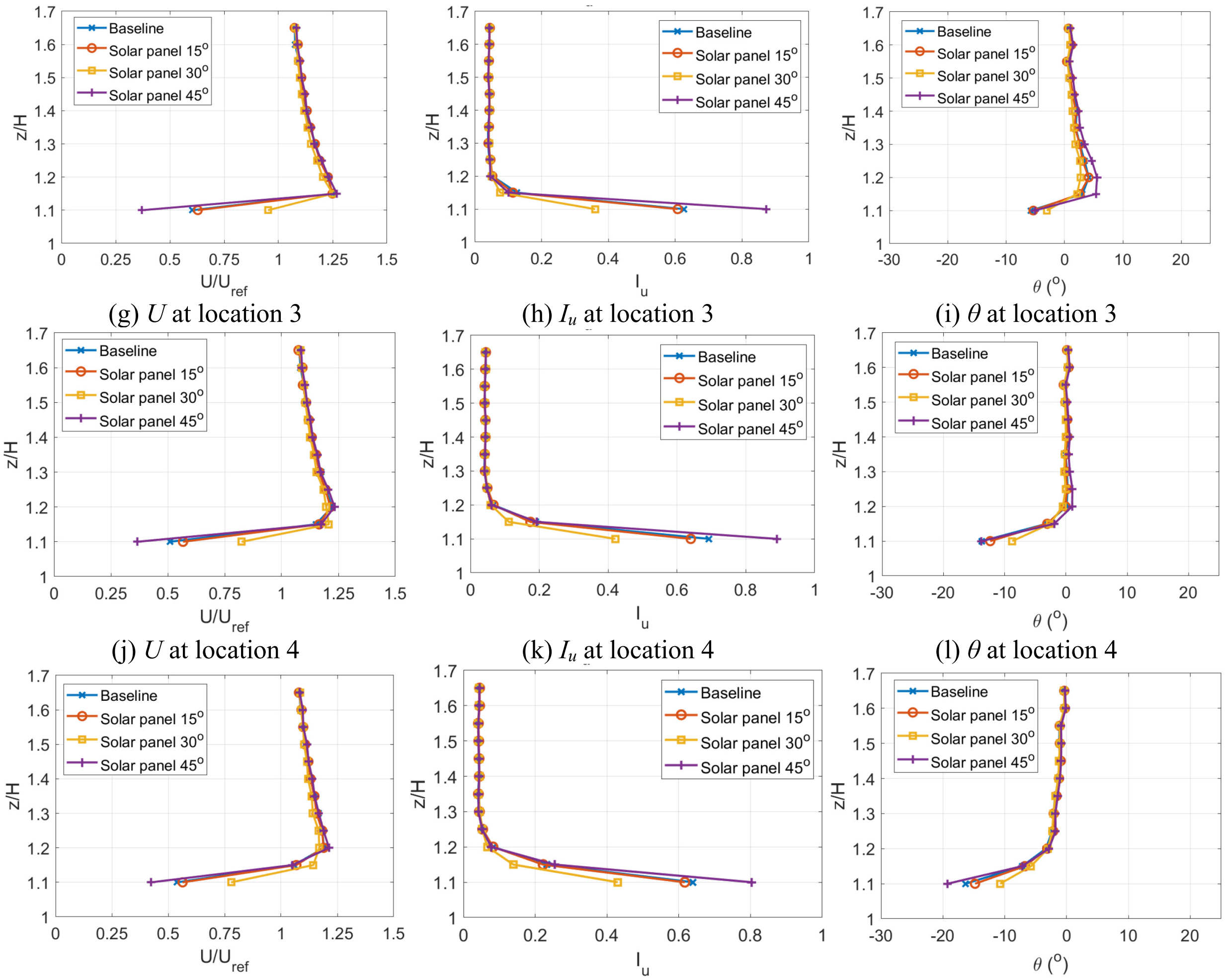

(g) U at location 3 (h) I_u at location 3 (i) θ at location 3

(j) U at location 4 (k) I_u at location 4 (l) θ at location 4

(m) U at location 5 (n) I_u at location 5 (o) θ at location 5

Figure 11. Rooftop flow characteristics for models with solar panel mounted on roof edge

306

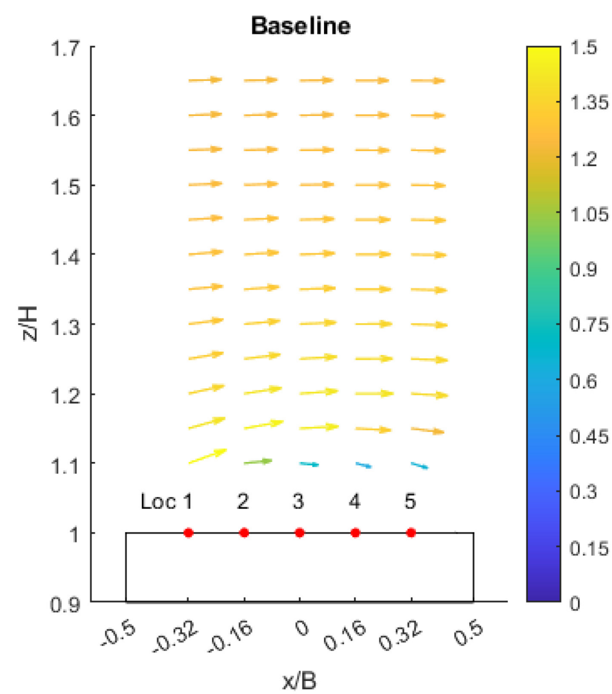

(a) Baseline model

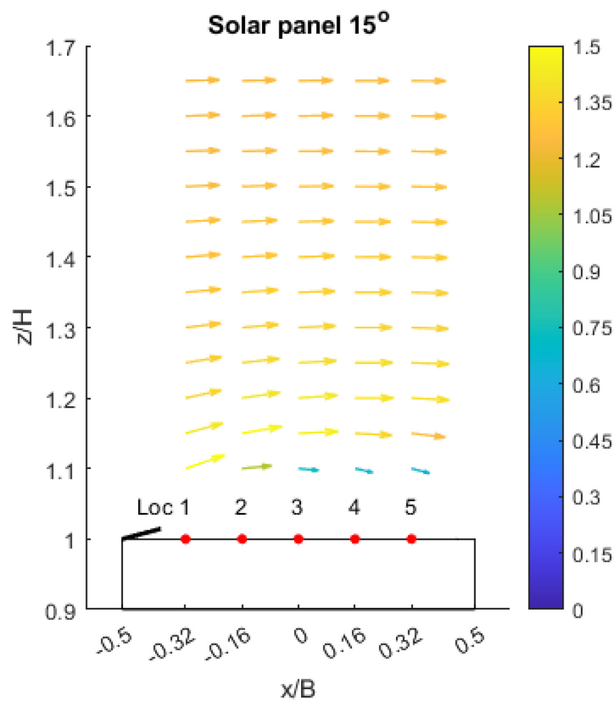

(b) Model with 15º solar panel

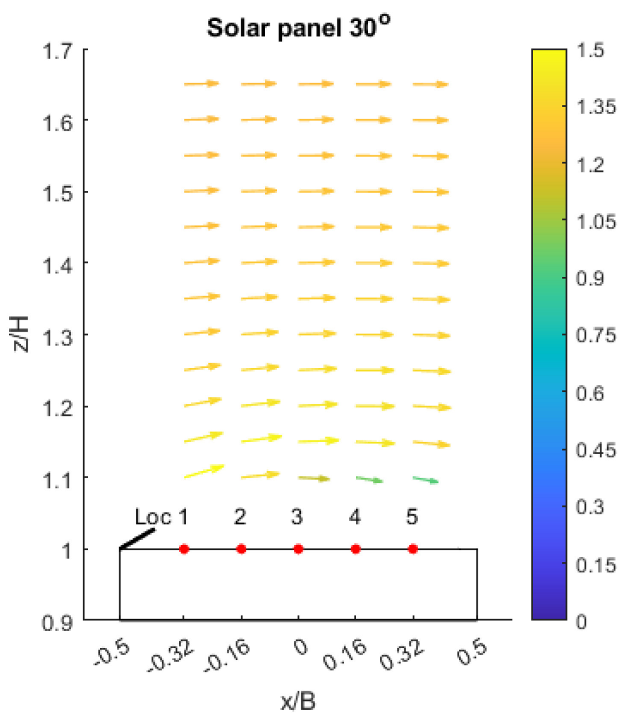

(c) Model with 30º solar panel

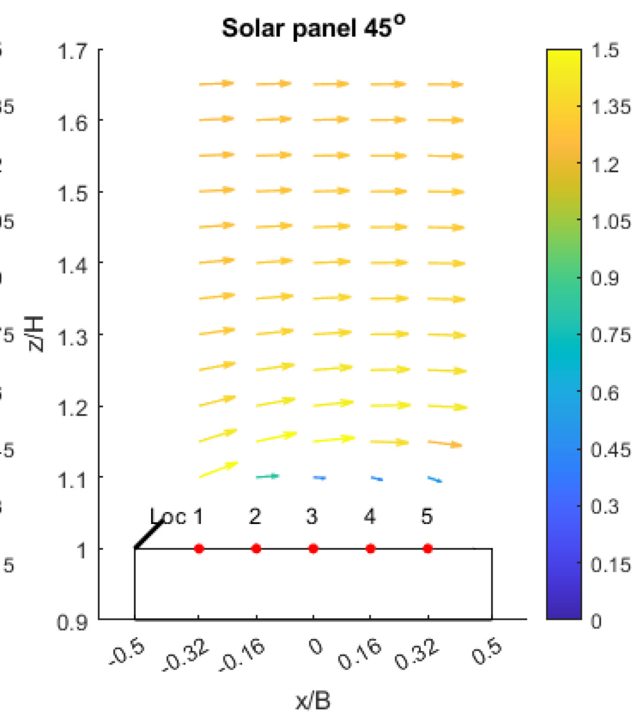

(d) Model with 45º solar panel

Figure 12. Vector-based mean wind field for models with solar panel mounted on roof edge

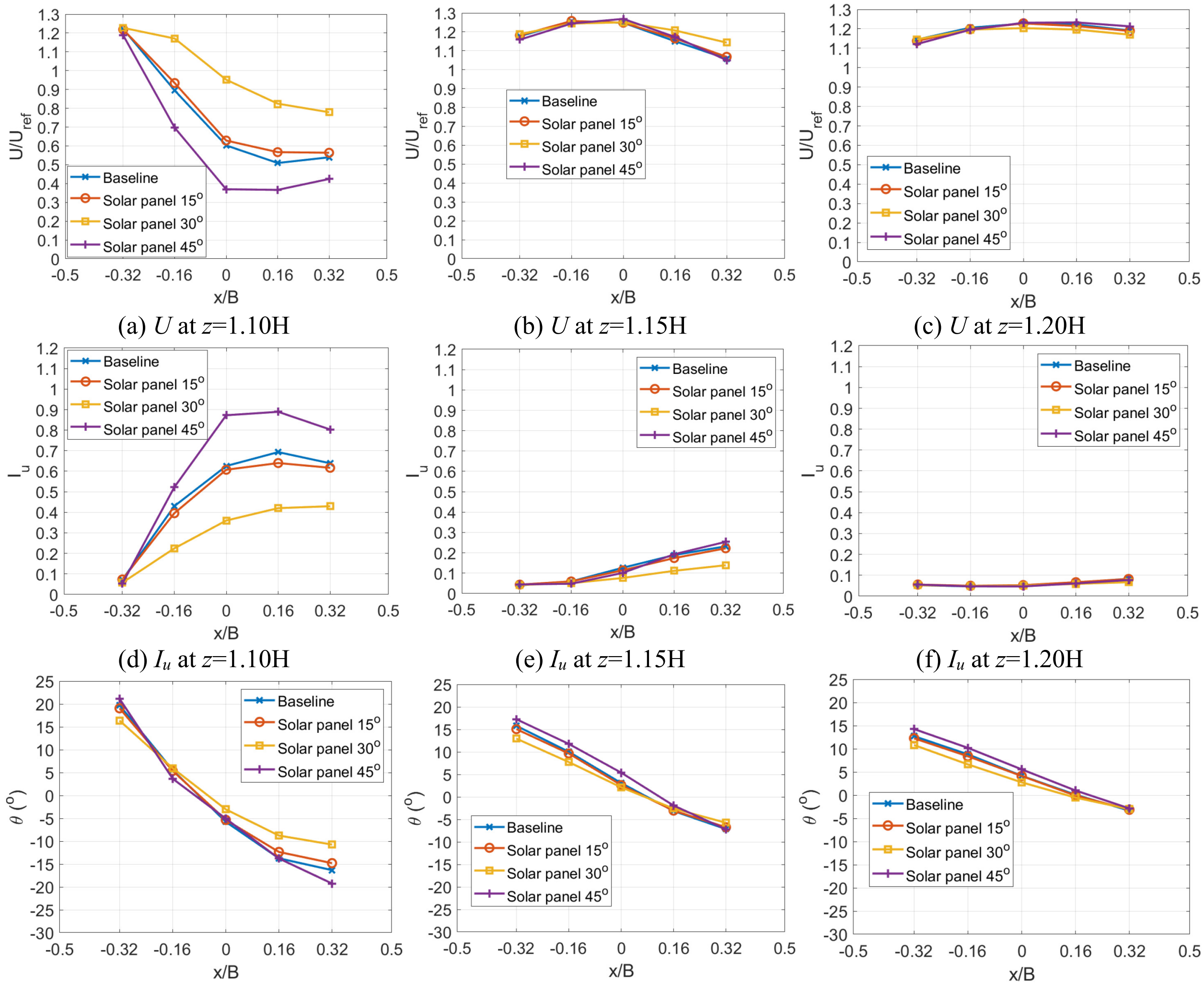

(a) U at z=1.10H (b) U at z=1.15H (c) U at z=1.20H

(d) I_u at z=1.10H (e) I_u at z=1.15H (f) I_u at z=1.20H

(g) θ at z=1.10H (h) θ at z=1.15H (i) θ at z=1.20H

Figure 13. Impact of solar panel (mounted on roof edge) on wind energy potential at z=1.10H, 1.15H and 1.20H

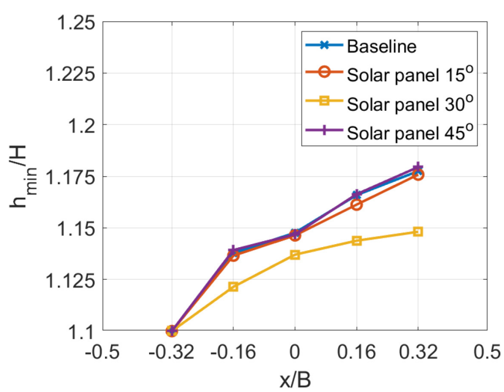

Figure 14. Impact of solar panel (mounted on roof edge) on minimum hub height h_{min}

3.2.2 *Solar panel mounted on parapet wall*

The scenarios of solar panel mounted on the top of parapet wall are investigated in this section, which aims to study the feasibility of using solar panel (or some type of active devices) to improve the wind energy potential for the case with only parapet wall (previously considered unfavorable for wind energy harvesting). The wind fields for model of the 40mm parapet wall (as the reference model) and solar panel mounted on the parapet wall (with tilting angle of 15º, 30º and 45º) are presented in Fig. 15, showing the mean wind speed U, turbulence intensity I_u and the skewness angle θ. The the vector-based representation of the mean wind field is shown in Fig. 16. It is noted that the impacts of solar panel are not as significant as that of solar panel mounted directly on the roof edge. Variations in U and I_u mainly occur near the roof, while the impact on θ can reach up to a higher elevation.

To clearly show the wind energy potential impacted by solar panel mounted on the parapet wall, the flow characteristics of three typical elevations at z = 1.10H, 1.15H and 1.20H are shown in Fig. 17. For the mean wind speed, 30º tilted solar angle can significantly contribute to increasing U at z = 1.10H and 1.15H, compared with the relatively small impact of 15º tilting angle and the general negative impact of 45º tilting angle. The impact of various tilting angles on U becomes insignificant at z = 1.20H. Regarding turbulence intensity, 30º tilted solar panel can effectively reduce I_u at both at z = 1.10H and 1.15H for all measurement locations, while 15º and 45º tilting angle generally have opposite effects on I_u at different elevations and measurement locations, which are not as promising compared to 30º tilting angle. The impact of tilting angle on I_u become less significant at a higher elevation of z = 1.20H. In terms of the skewness angle θ, 45º tilting angle seems to have the best performance at z = 1.10H, compared to that of 15º and 30º tilting angle. However, the reduced skewness angle θ from 45º tilting angle may be unimportant, considering the small value of mean wind speed U as shown in Fig. 17(a). On the other hand, 30º tilting angle can generally increase θ for z = 1.10H (except for the leeward location 5), while 15º tilting angle only increases θ for windward location 1 and 2. At higher elevations of z = 1.15H and 1.20H, the differences in θ resulting from various tilting angles are less significant, where only a slight improvement due to the 30º tilting angle is observed. The minimum hub heights h_{min} of horizontal-axis wind turbines are shown in Fig. 18 for models with different tilting angles. The obtained results clearly show that solar panel with 30º tilting angle has the best performance in terms of reducing the hub height for buildings with existing parapet wall, which also aligns with previous conclusion for the stand-alone solar panel on roof edge. The good performance of 30º tilted solar panel, mounted on the roof edge and on the parapet wall, confirms the promising potential of enhancing wind energy potentials through modifying the aerodynamic shape of building roof using active devices.

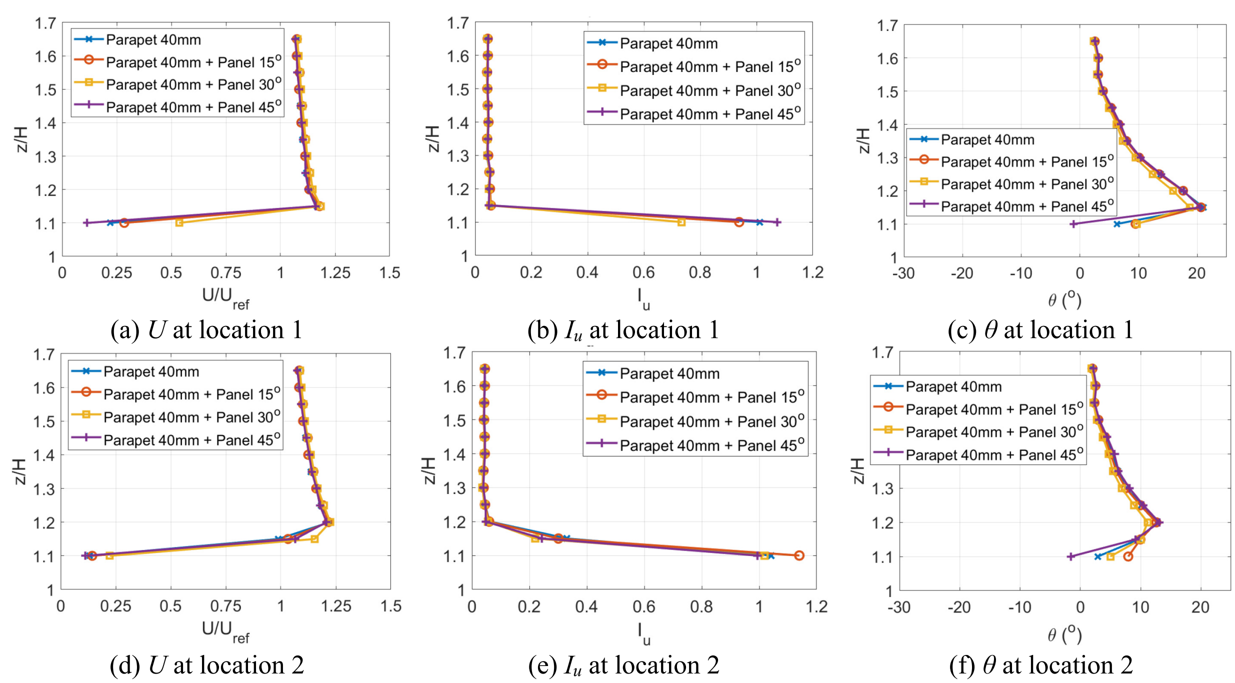

(a) U at location 1 (b) I_u at location 1 (c) θ at location 1

(d) U at location 2 (e) I_u at location 2 (f) θ at location 2

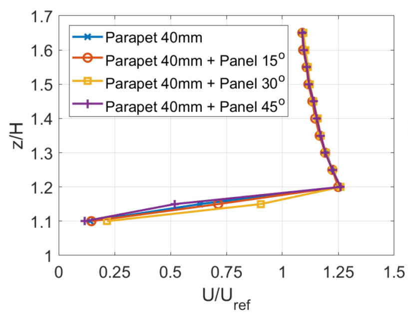

(g) U at location 3

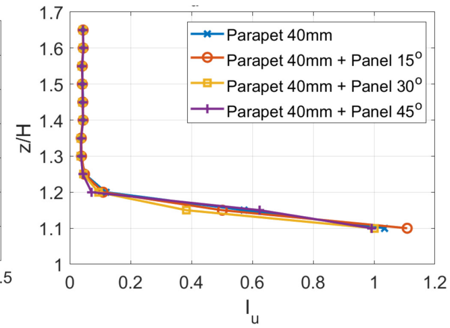

(h) I_u at location 3

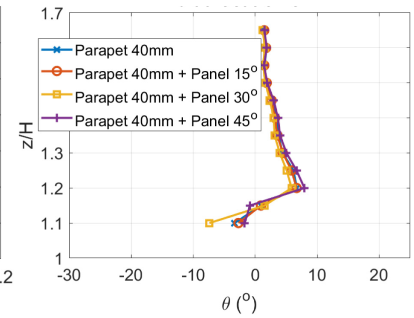

(i) θ at location 3

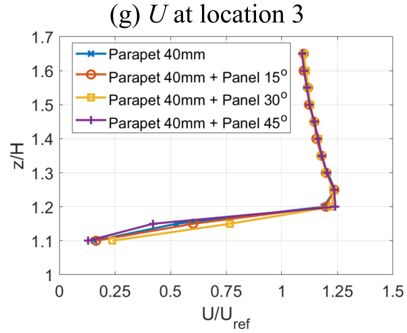

(j) U at location 4

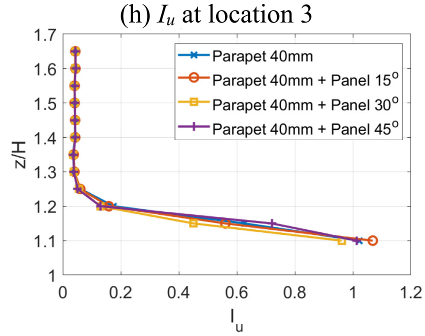

(k) I_u at location 4

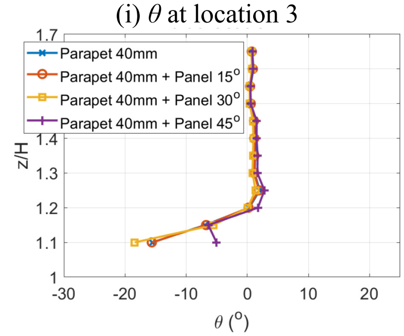

(l) θ at location 4

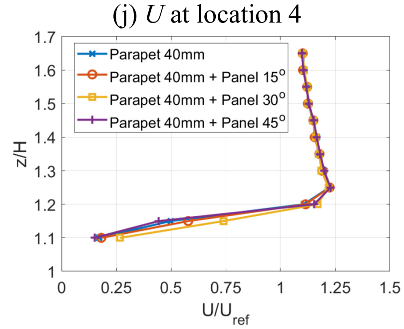

(m) U at location 5

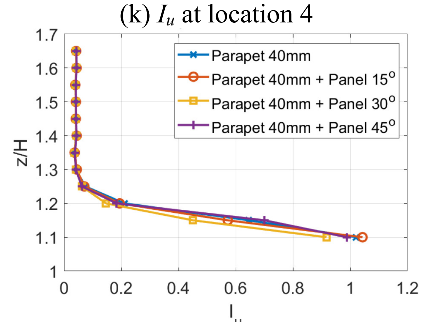

(n) I_u at location 5

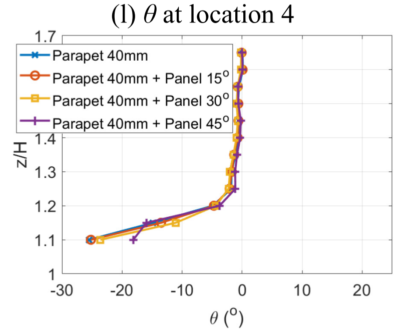

(o) θ at location 5

Figure 15. Rooftop flow characteristics for models with solar panel mounted on parapet wall

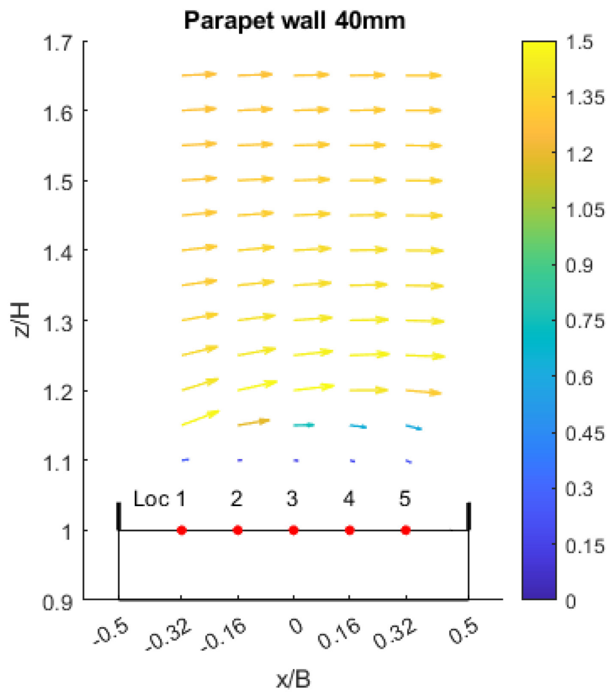

(a) Flow field for 40mm parapet wall

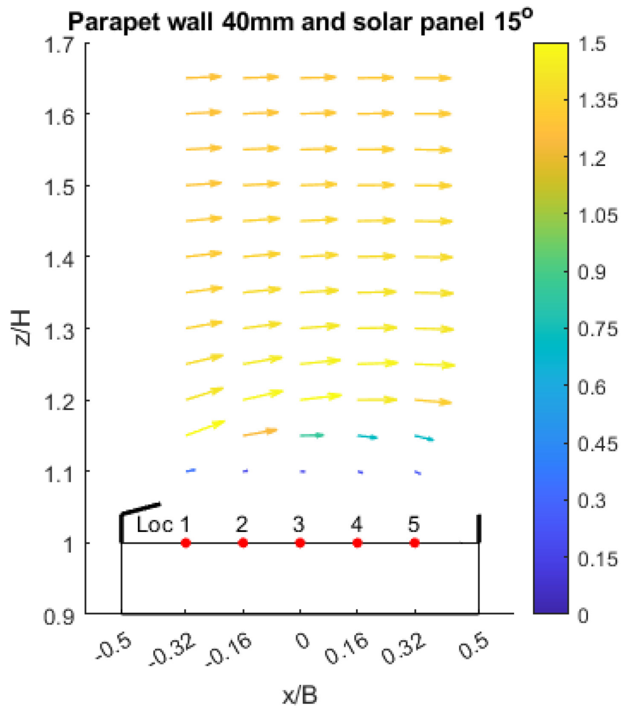

(b) Model with 40mm parapet wall and 15º solar panel

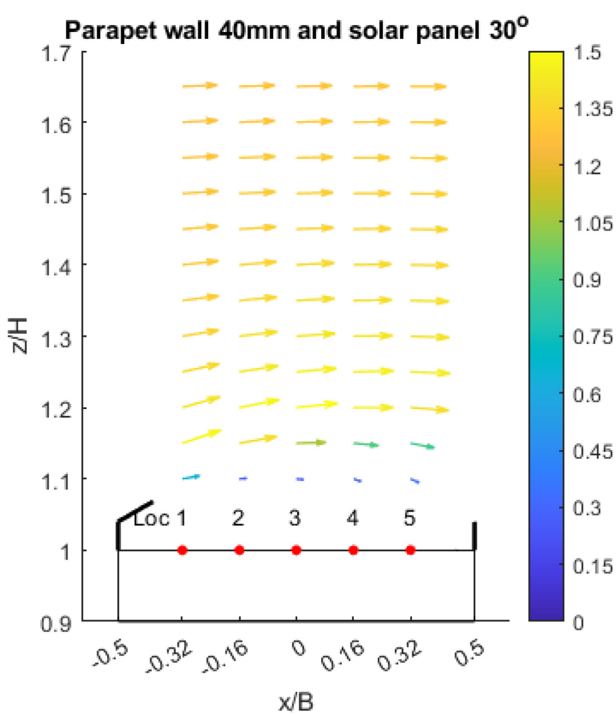

(c) Model with 40mm parapet wall and 30º solar panel

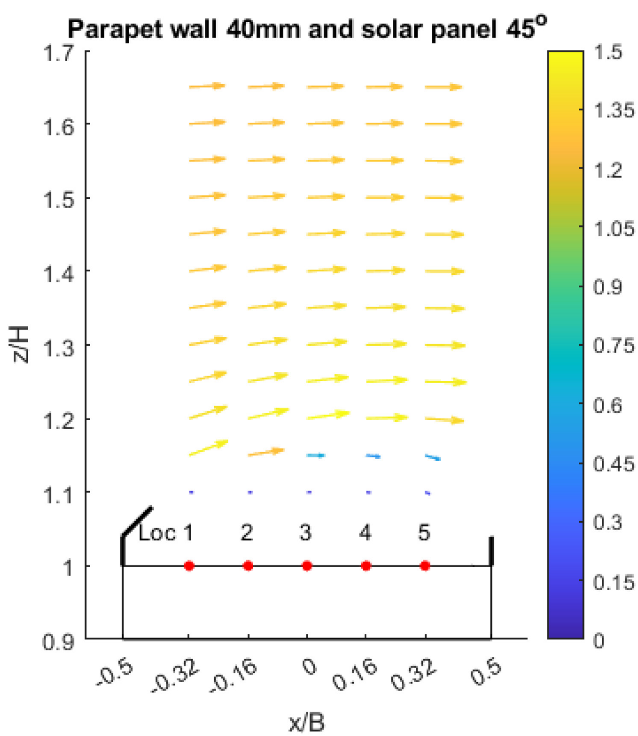

(d) Model with 40mm parapet wall and 45º solar panel

Figure 16. Vector-based mean wind field for models with solar panel mounted on parapet wall

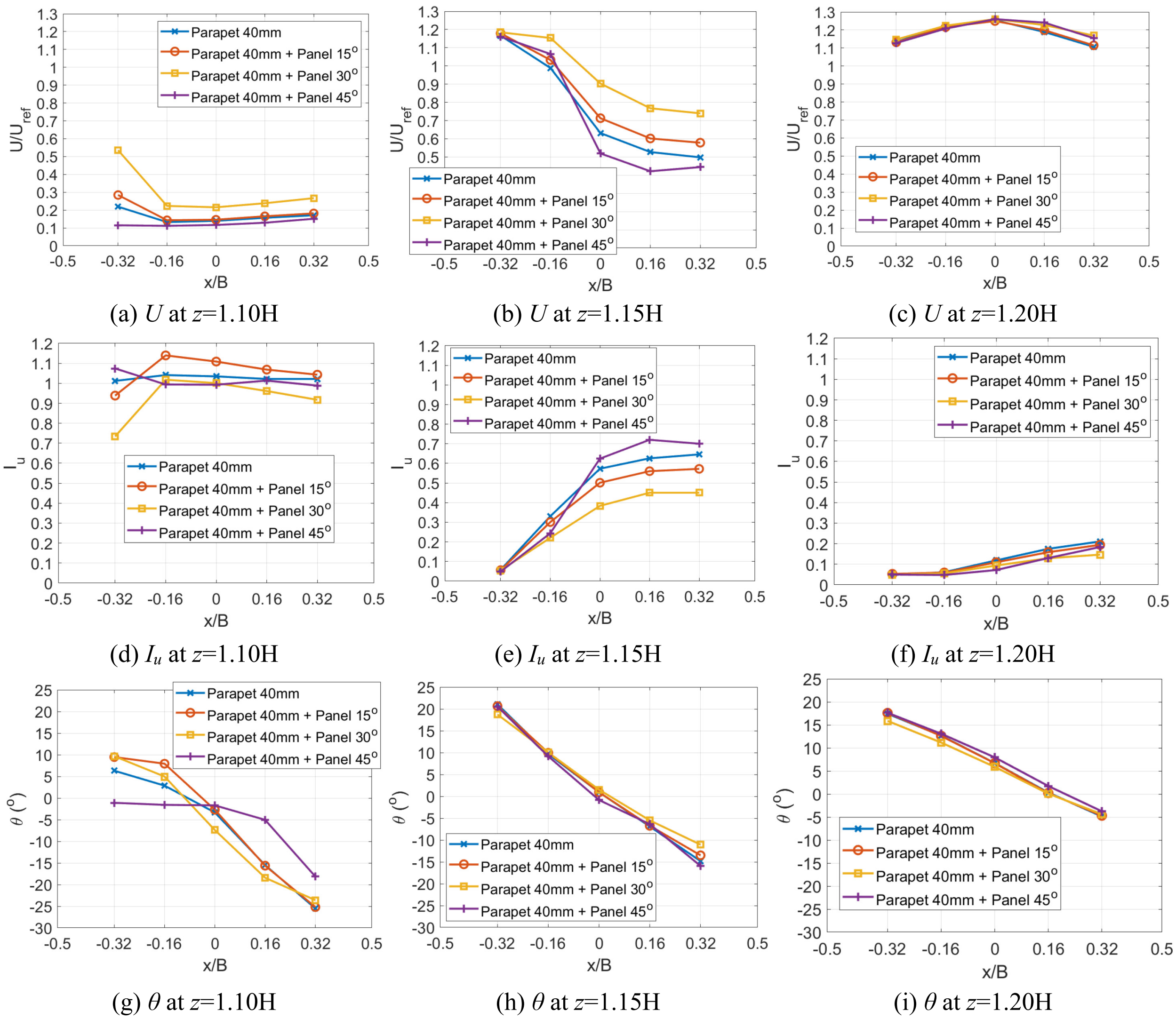

Figure 17. Impact of solar panel (mounted on parapet wall) on wind energy potential at z=1.10H, 1.15H and 1.20H

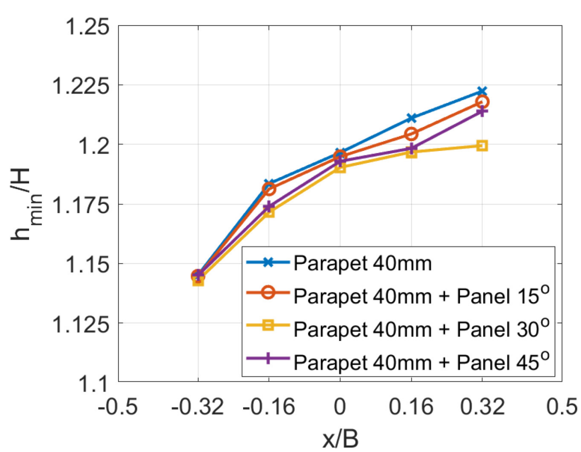

Figure 18. Impact of solar panel (mounted on parapet wall) on minimum hub height h_{min}

4 CONCLUDING REMARKS AND FUTURE DIRECTIONS

Wind tunnel tests are conducted in this study to investigate the flow characteristics and wind energy potential over flat building roofs with different edge configurations. In total, nine building configurations are tested in the wind tunnel, including one baseline model, two models with only parapet wall, three models with solar panel mounted on roof edge, and three models with solar panel mounted on parapet wall. Compared to the baseline model, the parapet wall generally slows down the wind speed and increases turbulence intensity as well as the skewness angle, which hence compromises the harvesting efficiency of wind energy. On the other hand, implementation of solar panel on the roof edge or on the top of parapet wall can modify the features of the flow separation and has the potential to enhance wind energy harvesting over the roof. Specifically, the promising configuration of 30º tilted solar panel is identified, which can generally increase mean wind speed and reduce turbulence intensity as well as the skewness angle. In addition to providing valuable data for validating CFD simulations, the obtained results in this study reveal the promising potential of using solar panels as active devices to adaptively change the roof shape for maximizing wind power generation. There are also some limitations in this study to be addressed in future work. Noting that only 0º wind direction is considered in the wind tunnel tests; further investigations covering a wide range of wind directions are desired in the future to better inform practical designs of wind energy harvesting devices. Also, this study only empirically identifies the promising 30º tilting angle of solar panels from a limited number of alternatives and for fixed approach flow conditions (both roughness and direction); it is ideal to search with a finer resolution or formulate it as an optimization problem. In addition, this study considers one row of solar panels on the windward roof edge to isolate their effects, which can be extended to more complex layouts in future studies. Lastly, the wind loads on the energy harvesting devices (both wind and solar) need to be assessed for practical implementation.

5 ACKNOWLEDGEMENTS

This material is based upon work supported by the National Science Foundation (NSF) under Grants No. 2028762 & 2028647. Any opinions, findings, and conclusions or recommendations expressed in this material are those of the authors and do not necessarily reflect the views of NSF.

APPENDIX

When measuring wind velocity using pressure-based probes, it is desirable that the instantaneous wind direction lies in the acceptance cone for measurement accuracy. In this study, the five-hole Vectoflow probes are used to measure the turbulent wind speed above the building roof, which has a ± 60º acceptance cone. Based on these considerations, the data quality is defined in this study as the percentage of samples whose instantaneous wind angle with respect to cobra probe tip orientation (i.e., *x* direction in Fig. 3) is smaller than 60º. The data quality for four representative cases (i.e., baseline, 40mm parapet wall, 30º solar panel, and the case with 30º solar panel sitting on 40mm parapet wall) are shown in Fig. A1. Note that only the measurement qualities for bottom two rows are shown here, above which the data qualities are all 100%. As shown in Fig. A1, the presence of parapet wall results in a drop in data quality, indicating a low mean velocity and recirculating flow (and hence poor wind energy potential). On the other hand, the existence of 30º solar panel can effectively enhance the data quality, potentially through increased mean wind speed and reduced turbulences. These observations in data quality reinforce the main conclusions of this study.

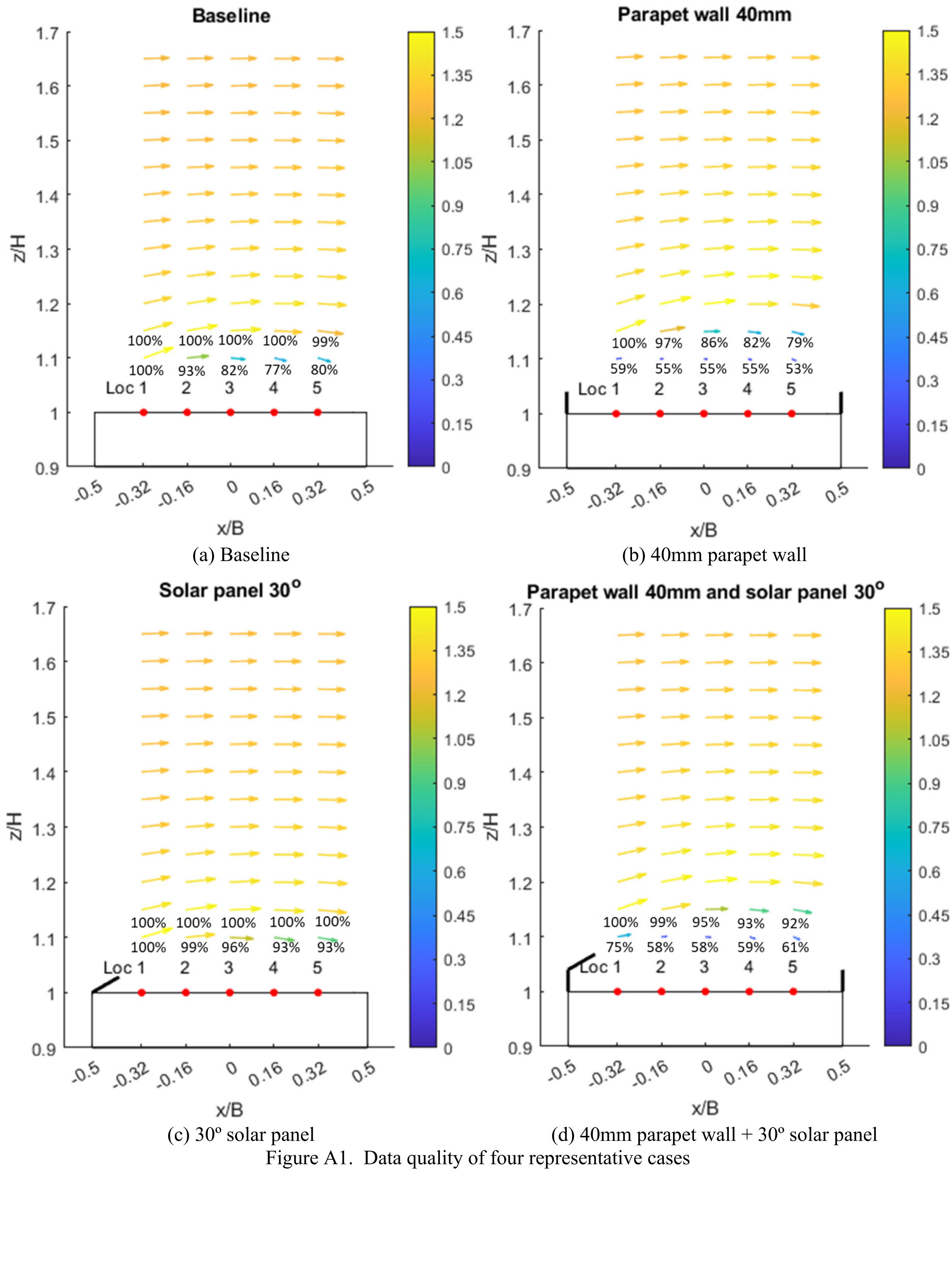

(a) Baseline (b) 40mm parapet wall

(c) 30º solar panel (d) 40mm parapet wall + 30º solar panel

Figure A1. Data quality of four representative cases

REFERENCES

Abdelkefi, A., 2016. Aeroelastic energy harvesting: A review. *International Journal of Engineering Science*, *100*, 112-135.

Ahmed, A., Ge, T., Peng, J., Yan, W.C., Tee, B.T. and You, S., 2022. Assessment of the renewable energy generation towards net-zero energy buildings: A review. *Energy and Buildings*, 256, 111755.

Anup, K.C., Whale, J. and Urmee, T., 2019. Urban wind conditions and small wind turbines in the built environment: A review. *Renewable energy*, 131, 268-283.

Catarelli, R.A., Fernández-Cabán, P.L., Masters, F.J., Bridge, J.A., Gurley, K.R. and Matyas, C.J., 2020a. Automated terrain generation for precise atmospheric boundary layer simulation in the wind tunnel. *Journal of Wind Engineering and Industrial Aerodynamics*, 207, 104276.

Catarelli, R.A., Fernández-Cabán, P.L., Phillips, B.M., Bridge, J.A., Masters, F.J., Gurley, K.R. and Prevatt, D.O., 2020b. Automation and new capabilities in the university of Florida NHERI Boundary Layer Wind Tunnel. *Frontiers in Built Environment*, 6, 558151.

Dai, S.F., Liu, H.J., Chu, Y.J., Lam, H.F. and Peng, H.Y., 2022a. Impact of corner modification on wind characteristics and wind energy potential over flat roofs of tall buildings. *Energy*, 241, 122920.

Dai, S.F., Liu, H.J. and Peng, H.Y., 2022b. Assessment of parapet effect on wind flow properties and wind energy potential over roofs of tall buildings. *Renewable Energy*, 199, 826-839.

Dai, S.F., Liu, H.J., Yang, J.H. and Peng, H.Y., 2022c. Wind loads on roof-mounted isolated solar panels of tall buildings through wind tunnel testing. *Solar Energy*, 231, 607-622.

Ellabban, O., Abu-Rub, H. and Blaabjerg, F., 2014. Renewable energy resources: Current status, future prospects and their enabling technology. *Renewable and sustainable energy reviews*, 39, 748-764.

Glumac, A.Š., Hemida, H. and Höffer, R., 2018. Wind energy potential above a high-rise building influenced by neighboring buildings: An experimental investigation. *Journal of Wind Engineering and Industrial Aerodynamics*, 175, 32-42.

Hassanli, S., Hu, G., Kwok, K.C. and Fletcher, D.F., 2017. Utilizing cavity flow within double skin façade for wind energy harvesting in buildings. *Journal of Wind Engineering and Industrial Aerodynamics*, 167, 114-127.

Hong, C.M. and Chen, C.H., 2014. Intelligent control of a grid-connected wind-photovoltaic hybrid power systems. *International Journal of Electrical Power & Energy Systems*, 55, 554-561.

Huang, Q., Shi, Y., Wang, Y., Lu, L. and Cui, Y., 2015. Multi-turbine wind-solar hybrid system. *Renewable Energy*, 76, 401-407.

IPCC, 2023. Climate Change 2023: Synthesis Report of the IPCC Sixth Assessment Report. https://www.ipcc.ch/report/ar6/syr/downloads/report/IPCC_AR6_SYR_LongerReport.pdf, Accessed on June 20, 2023.

Jafari, S.A.H., Kwok, K.C., Safaei, F., Kosasih, B. and Zhao, M., 2019. Aerodynamic analysis of a stator-augmented linear cascade wind turbine. *Wind Energy*, 22(8), 1148-1163.

Juan, Y.H., Wen, C.Y., Li, Z. and Yang, A.S., 2021. Impacts of urban morphology on improving urban wind energy potential for generic high-rise building arrays. *Applied Energy*, 299, 117304.

Juan, Y.H., Rezaeiha, A., Montazeri, H., Blocken, B., Wen, C.Y. and Yang, A.S., 2022. CFD assessment of wind energy potential for generic high-rise buildings in close proximity: Impact of building arrangement and height. *Applied Energy*, 321, 119328.

Kono, T., Kogaki, T. and Kiwata, T., 2016. Numerical investigation of wind conditions for roof-mounted wind turbines: effects of wind direction and horizontal aspect ratio of a high-rise cuboid building. *Energies*, 9(11), 907.

Kumar, R., Raahemifar, K. and Fung, A.S., 2018. A critical review of vertical axis wind turbines for urban applications. *Renewable and Sustainable Energy Reviews*, 89, 281-291.

Kwok, K.C.S. and Hu, G., 2023. Wind energy system for buildings in an urban environment. *Journal of Wind Engineering and Industrial Aerodynamics*, 234, 105349.

Lai, Z., Wang, S., Zhu, L., Zhang, G., Wang, J., Yang, K. and Yurchenko, D., 2021. A hybrid piezo-dielectric wind energy harvester for high-performance vortex-induced vibration energy harvesting. *Mechanical Systems and Signal Processing*, 150, 107212.

Li, Q.S., Chen, F.B., Li, Y.G. and Lee, Y.Y., 2013. Implementing wind turbines in a tall building for power generation: A study of wind loads and wind speed amplifications. *Journal of Wind Engineering and Industrial Aerodynamics*, 116, 70-82.

Liu, L.Q. and Wang, Z.X., 2009. The development and application practice of wind–solar energy hybrid generation systems in China. *Renewable and Sustainable Energy Reviews*, 13(6-7), 1504-1512.

Lu, L. and Ip, K.Y., 2009. Investigation on the feasibility and enhancement methods of wind power utilization in high-rise buildings of Hong Kong. *Renewable and Sustainable Energy Reviews*, 13(2), 450-461.

Moss, R.H., Edmonds, J.A., Hibbard, K.A., Manning, M.R., Rose, S.K., Van Vuuren, D.P., Carter, T.R., Emori, S., Kainuma, M., Kram, T. and Meehl, G.A., 2010. The next generation of scenarios for climate change research and assessment. *Nature*, 463(7282), 747-756.

Peng, H.Y., Dai, S.F., Lin, K., Hu, G. and Liu, H.J., 2020. Experimental investigation of wind characteristics and wind energy potential over rooftops: Effects of building parameters. *Journal of Wind Engineering and Industrial Aerodynamics*, 205, 104304.

Pierik, J.T.G., Dekker, J.W.M., Braam, H., Bulder, B.H., Winkelaar, D., Larsen, G.C., 1999. Wind energy for the next millennium. In: *Proceedings of the European Wind Turbine Standards II (EWTS-II)*. James and James Science Publishers, London.

Pratt, R.N. and Kopp, G.A., 2013. Velocity measurements around low-profile, tilted, solar arrays mounted on large flat-roofs, for wall normal wind directions. *Journal of Wind Engineering and Industrial Aerodynamics*, 123, 226-238.

Sinha, S., Chandel, S.S. and Malik, P., 2021. Investigation of a building-integrated solar photovoltaic-wind-battery hybrid energy system: A case study. *International Journal of Energy Research*, 45(15), 21534-21539.

Škvorc, P. and Kozmar, H., 2021. Wind energy harnessing on tall buildings in urban environments. *Renewable and Sustainable Energy Reviews*, 152, 111662.

Stathopoulos, T., Zisis, I. and Xypnitou, E., 2014. Local and overall wind pressure and force coefficients for solar panels. *Journal of wind engineering and industrial aerodynamics*, 125, 195-206.

Stathopoulos, T., Alrawashdeh, H., Al-Quraan, A., Blocken, B., Dilimulati, A., Paraschivoiu, M. and Pilay, P., 2018. Urban wind energy: Some views on potential and challenges. *Journal of Wind Engineering and Industrial Aerodynamics*, 179, 146-157.

Toja-Silva, F., Colmenar-Santos, A. and Castro-Gil, M., 2013. Urban wind energy exploitation systems: Behaviour under multidirectional flow conditions—Opportunities and challenges. *Renewable and Sustainable Energy Reviews*, 24, 364-378.

Toja-Silva, F., Peralta, C., Lopez-Garcia, O., Navarro, J. and Cruz, I., 2015a. Roof region dependent wind potential assessment with different RANS turbulence models. *Journal of Wind Engineering and Industrial Aerodynamics*, 142, 258-271.

Toja-Silva, F., Peralta, C., Lopez-Garcia, O., Navarro, J. and Cruz, I., 2015b. Effect of roof-mounted solar panels on the wind energy exploitation on high-rise buildings. *Journal of Wind Engineering and Industrial Aerodynamics*, 145, 123-138.

Toja-Silva, F., Lopez-Garcia, O., Peralta, C., Navarro, J. and Cruz, I., 2016. An empirical–heuristic optimization of the building-roof geometry for urban wind energy exploitation on high-rise buildings. *Applied energy*, 164, 769-794.

Toja-Silva, F., Kono, T., Peralta, C., Lopez-Garcia, O. and Chen, J., 2018. A review of computational fluid dynamics (CFD) simulations of the wind flow around buildings for urban wind energy exploitation. *Journal of Wind Engineering and Industrial Aerodynamics*, 180, 66-87.

Vectoflow, https://vectoflow.de/en, Accessed on June 20, 2023.

Vita, G., Šarkić-Glumac, A., Hemida, H., Salvadori, S. and Baniotopoulos, C., 2020a. On the wind energy resource above high-rise buildings. *Energies*, 13(14), 3641.

Vita, G., Hashmi, S.A., Salvadori, S., Hemida, H. and Baniotopoulos, C., 2020b. Role of inflow turbulence and surrounding buildings on large eddy simulations of urban wind energy. *Energies*, 13(19), 5208.

Wang, B., Cot, L.D., Adolphe, L., Geoffroy, S. and Morchain, J., 2015. Estimation of wind energy over roof of two perpendicular buildings. *Energy and Buildings*, 88, 57-67.

Wang, J., Van Phuc, P., Yang, Q. and Tamura, Y., 2020. LES study of wind pressure and flow characteristics of flat-roof-mounted solar arrays. *Journal of Wind Engineering and Industrial Aerodynamics*, 198, 104096.